Supporting Information for

Coupled impact of proteins with different molecular weights and surface charges on TiO2 mobility

Chaorui Yan[a], Prabhakar Sharma[b], Qing Chen[c], Baoguo Li[a], Jianying Shang[a] *

[a] Key Laboratory of Plant-Soil Interactions, Ministry of Education, Key Laboratory of Arable Land Conservation (North China), Ministry of Agriculture, College of Land Science and Technology, China Agricultural University, Beijing 100193, P. R. China

[b] School of Ecology and Environment Studies, Nalanda University, Rajgir, Nalanda, Bihar, India

[c] College of Resources and Environmental Sciences, China Agricultural University, Beijing, 100193, China

* Corresponding author: Tel: +86 10 62733509; Fax: +86 10 62733509;

E-mail address: jyshang@cau.edu.cn

Contents

18 pages, 16 figures, and 2 tables

Contents

Table S1 Hydrodynamic diameters (D_H) of TiO_2, TiO_2 with different BSA concentrations, and TiO_2 with different proteins in suspensions prior to and at the end of the column experiment. (Page 17)
Table S2 Charge density (ZN/N_A), adsorbed layer thickness (d), and softness parameter ($1/\lambda$) are estimated by fitting electrophoretic mobility with the Ohshima's soft particle theory. (Page 18)

XDLVO Calculations

Interaction energy profiles of TiO_2 with proteins were calculated by XDLVO theory. Calculation equations of TiO_2-TiO_2 and TiO_2-sand were as follows (Einarson et al., 1993; Shang et al., 2010; Song et al., 2011; Sun et al., 2015; Xu et al., 2017):

$$\Phi_{\text{VDW-SS}} = -\frac{A_{121}}{6}\left[\frac{2R^2}{H(4R+H)} + \frac{2R^2}{(2R+H)^2} + \ln\frac{H(4R+H)}{(2R+H)^2}\right] \quad \text{(S1)}$$

$$\Phi_{\text{VDW-SP}} = -\frac{A_{123}R}{6h}\left[1 - \frac{5.32h}{\lambda_0}\ln\left(1 + \frac{\lambda_0}{5.32h}\right)\right] \quad \text{(S2)}$$

$$\Phi_{\text{EDL-SS}} = 32\pi\varepsilon_0\varepsilon_{\text{w}}R\gamma_1^2\left(\frac{k_{\text{B}}T}{zq}\right)^2 e^{-\kappa H} \quad \text{(S3)}$$

$$\Phi_{\text{EDL-SP}} = 64\pi\varepsilon_0\varepsilon_w R\gamma_1\gamma_2\left(\frac{k_{\text{B}}T}{zq}\right)^2 e^{-\kappa h} \quad \text{(S4)}$$

$$\kappa^{-1} = \sqrt{\frac{\varepsilon_0\varepsilon_w k_{\text{B}}T}{2N_A I q^2}} \quad \text{(S5)}$$

$$\gamma_1 = \tanh\left(\frac{zq\xi_1}{4k_{\text{B}}T}\right) \quad \text{(S6)}$$

$$\gamma_2 = \tanh\left(\frac{zq\xi_2}{4k_{\text{B}}T}\right) \quad \text{(S7)}$$

$$\Phi_{\text{OSM-SS}} = 0 \qquad 2d \le H \quad \text{(S8)}$$

$$\Phi_{\text{OSM-SS}} = \frac{4\pi R N_{\text{A}}}{V}\phi_{\text{P}}^2\left(\frac{1}{2} - \chi\right)\left(d - \frac{H}{2}\right)^2 \qquad d \le H \le 2d \quad \text{(S9)}$$

$$\Phi_{\text{OSM-SS}} = \frac{4\pi R N_{\text{A}}}{V}\phi_{\text{P}}^2\left(\frac{1}{2} - \chi\right)d^2\left[\frac{H}{2d} - \frac{1}{4} - \ln\left(\frac{H}{d}\right)\right] \qquad 0 < H < d \quad \text{(S10)}$$

$$\Phi_{\text{ELAS-SS}} = 0 \qquad d \leq H \quad \text{(S11)}$$

$$\Phi_{\text{ELAS-SS}} = \frac{2\pi R N_{\text{A}}}{M_{\text{W}}} \phi_{\text{P}} d^2 \rho \left\{ \frac{H}{d} \ln\left[\frac{H}{d} \left(\frac{3 - \frac{H}{d}}{2} \right)^2 \right] - 6 \ln\left(\frac{3 - \frac{H}{d}}{2} \right) + 3\left(1 - \frac{H}{d}\right) \right\} \qquad H < d \quad \text{(S12)}$$

$$\Phi_{\text{OSM-SP}} = \frac{2\pi R N_{\text{A}}}{V} \phi_{\text{P}}^2 \left(\frac{1}{2} - \chi \right) (d - h)^2 \qquad d > h > 0 \quad \text{(S13)}$$

$$\Phi_{\text{ELAS-SP}} = \frac{2\pi R N_{\text{A}}}{M_{\text{W}}} \phi_{\text{P}} d^2 \rho \left[\frac{2}{3} - \frac{1}{6}\left(\frac{h}{d}\right)^3 - \left(\frac{h}{2d}\right) + \left(\frac{h}{d}\right) \ln\left(\frac{h}{d}\right) \right] \qquad d > h > 0 \quad \text{(S14)}$$

$$\phi_{\text{P}} = \frac{3\Gamma_{\max} R^2}{\rho\left[(d + R)^3 - R^3 \right]} \qquad \text{(S15)}$$

$$\Phi_{\text{Total-XDLVO}} = \Phi_{\text{VDW}} + \Phi_{\text{EDL}} + \Phi_{\text{OSM}} + \Phi_{\text{ELAS}} \qquad \text{(S16)}$$

where A_{121} is the Hamaker constant for TiO_2-water-TiO_2, A_{123} is the Hamaker constant for TiO_2-water-sand, H is the separation distance between TiO_2 and TiO_2, h is separation distance between TiO_2 and sand surface, λ_0 is a characteristic length of 100 nm, ε_0 is the dielectric permittivity of vacuum, ε_w is the dielectric constant of water, N_A is Avogadro constant, χ is the Flory-Huggins solvency parameter, V is the molar volume of water, ϕ_P is the volume fraction of the protein, Γ_{max} is maximum surface concentration, ρ is the density of the protein, M_W is the molecular weight of the protein, Φ_{VDW} is van der Waals interaction energies, Φ_{EDL} is electrical double layer interaction energies, Φ_{OSM} is osmotic pressure, Φ_{ELAS} is elastic-steric repulsion.

References

Einarson, M.B., Berg, J.C., 1993. Electrosteric stabilization of colloidal latex dispersions. J. Colloid Interf. Sci. 155(1): 165-172.

Shang, J.Y., Liu, C.X., Wang, Z.M., Wu, H., Zhu, K.K., Li, J., Liu, J., 2010. In-situ measurements of engineered nanoporous particle transport in saturated porous media. Environ. Sci. Technol. 44(21): 8190-8195.

Song, J.E., Phenrat, T., Marinakos, S., Xiao, Y., Liu, J., Wiesner, M.R., Tilton, R.D., Lowry, G.V., 2011. Hydrophobic interactions increase attachment of gum Arabic- and PVP-coated Ag nanoparticles to hydrophobic surfaces. Environ. Sci. Technol. 45(14): 5988-5995.

Sun, P., Zhang, K.K., Fang, J., Lin, D.H., Wang, M.H., Han, J.Y., 2015. Transport of TiO2 nanoparticles in soil in the presence of surfactants. Sci. Total Environ. 527-528: 420-428.

Xu, S., Attinti, R., Adams, E., Wei, J., Kniel, K., Zhuang, J., Jin, Y., 2017. Mutually facilitated co-transport of two different viruses through reactive porous media. Water Res. 123: 40-48.

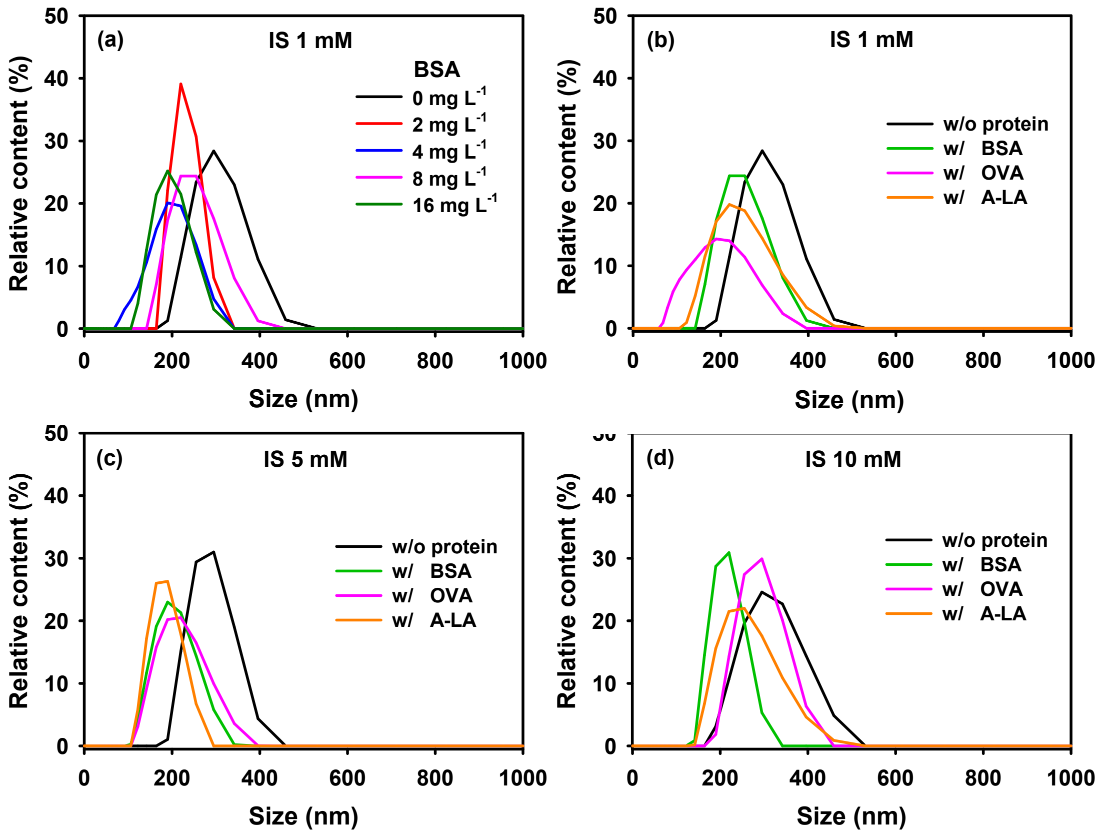

Fig. S1 The particle size distribution profiles of TiO_2 in the absence/presence of protein at different IS.

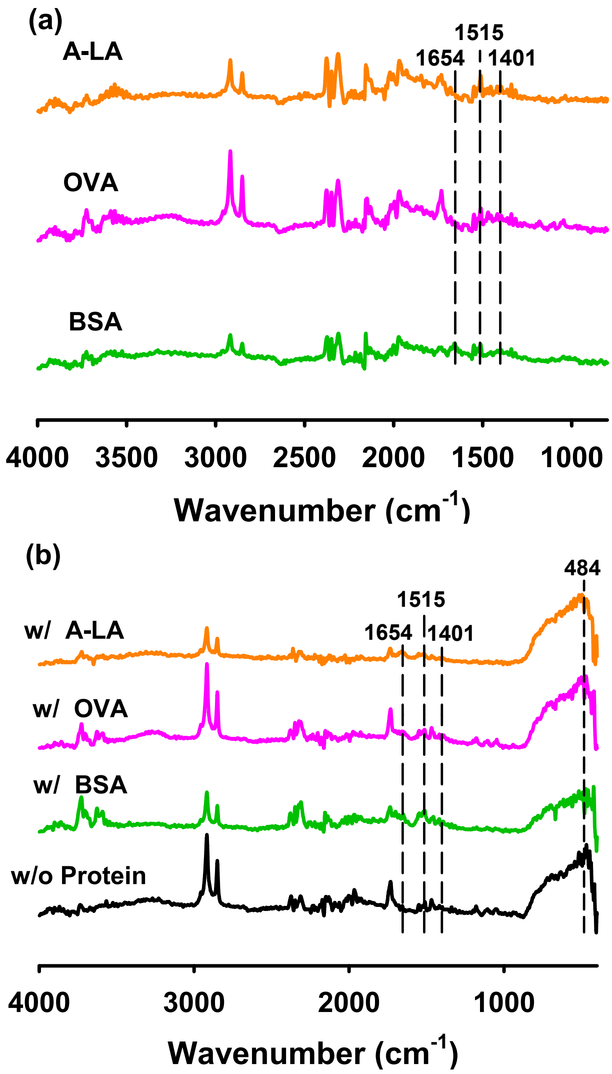

Fig. S2 ATR-FTIR spectra of 8 mg L^{-1} different proteins (a), TiO_2 without/with 8 mg L^{-1} BSA, OVA, and A-LA (b).

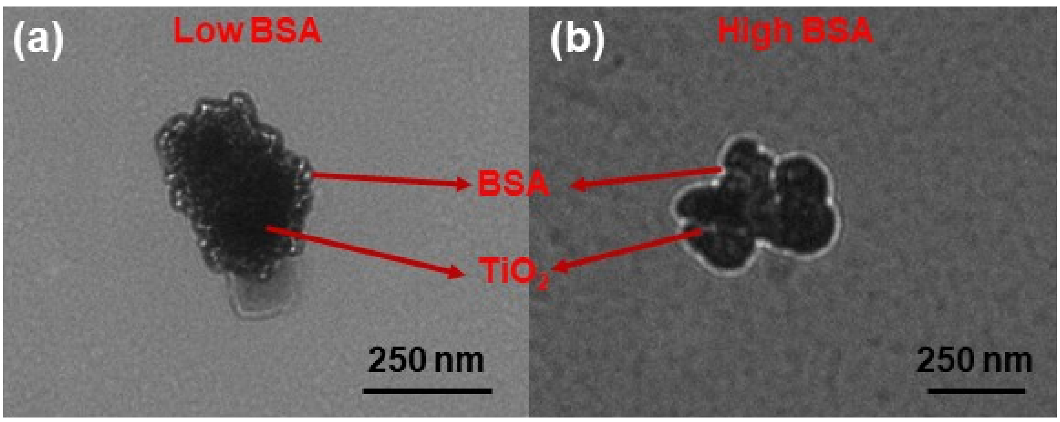

Fig. S3 TEM images of (a) TiO_2 with 4 mg L^{-1} BSA concentration, and (b) TiO_2 with 16 mg L^{-1} BSA concentration at IS 1 mM. The dark color is TiO_2, and the white layer is the adsorption layer of protein.

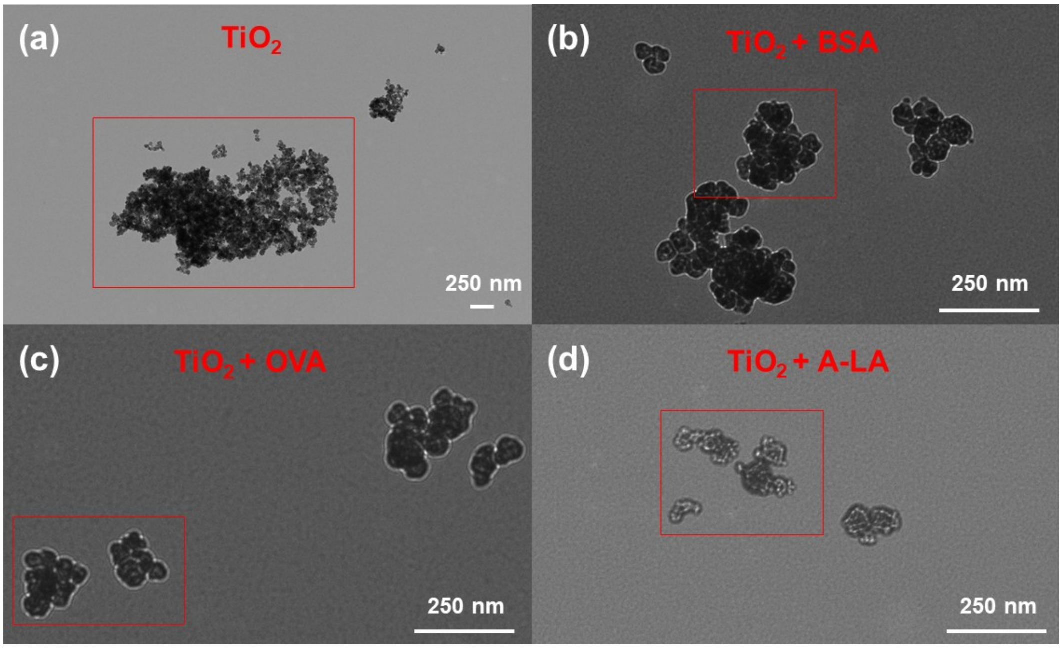

Fig. S4 TEM images of TiO_2 in the (a) absence and presence of 8 mg L^{-1} (b) BSA, (c) OVA, and (c) A-LA in IS 5 mM NaCl solution. The red area is the enlarged images, shown in Fig. 4.

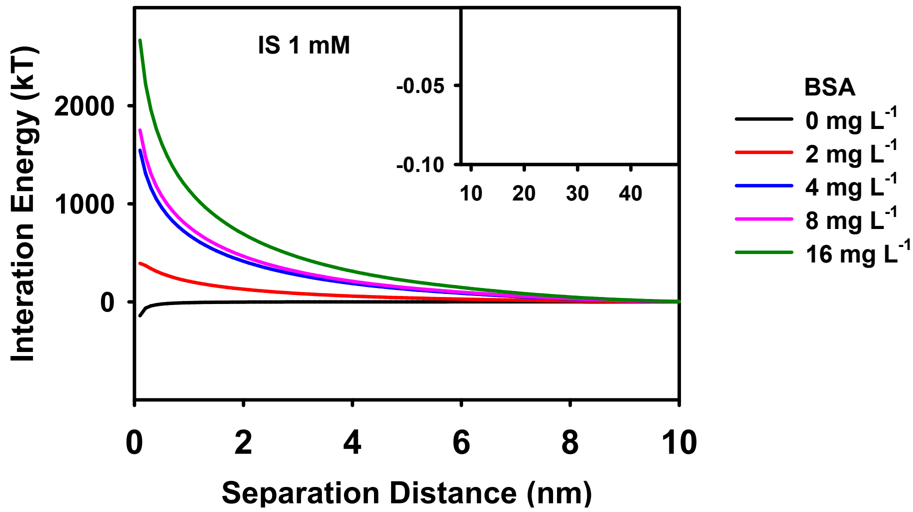

Fig. S5 Interaction energy profiles between TiO_2 with different BSA concentrations at IS 1 mM.

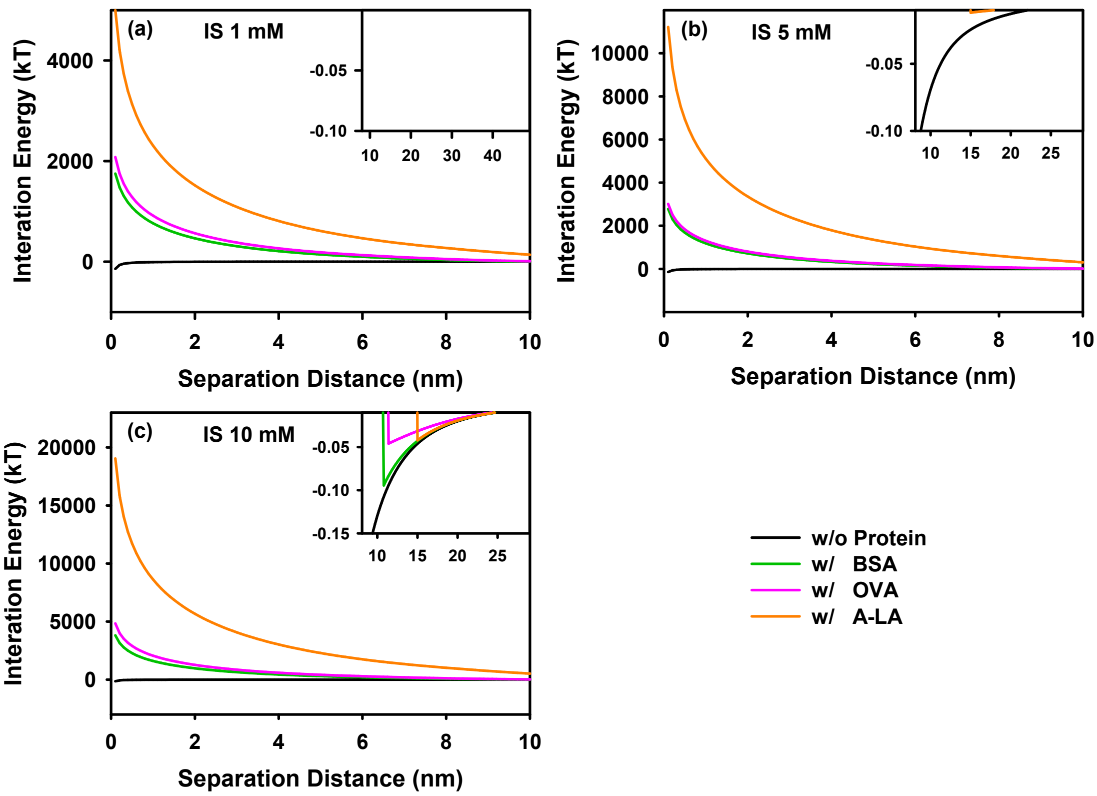

Fig. S6 Interaction energy profiles between TiO_2 with 8 mg L^{-1} different protein (BSA/OVA/A-LA) at different IS.

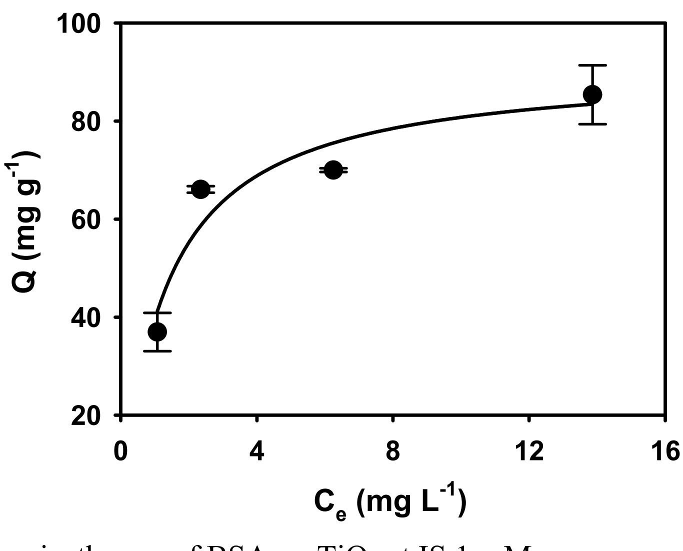

Fig. S7 Adsorption isotherms of BSA on TiO_2 at IS 1 mM.

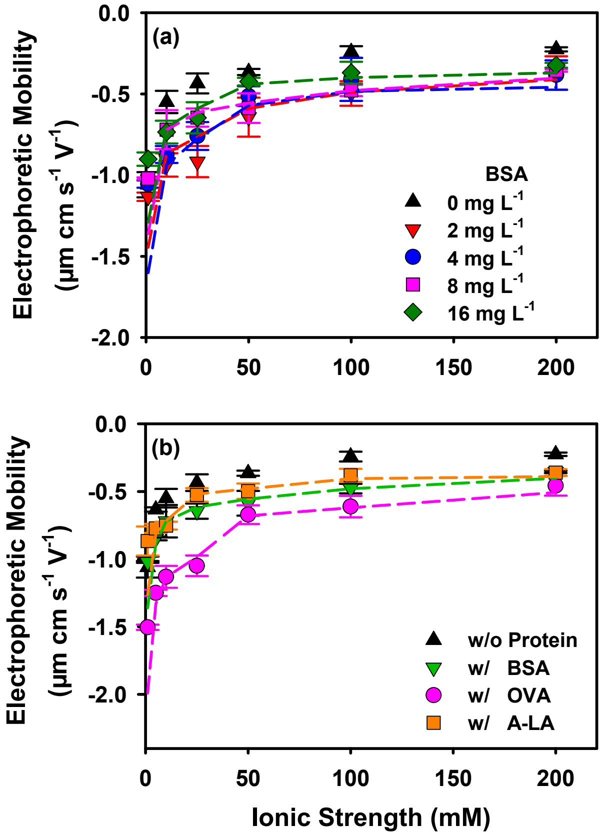

Fig. S8 Electrophoretic mobility (EPM) of TiO_2 in the presence of different proteins at different IS (1, 5, 25, 50, 100, and 200 mM) for pH 7. The dashed lines connect the best-fitted points with the Ohshima's soft particle theory.

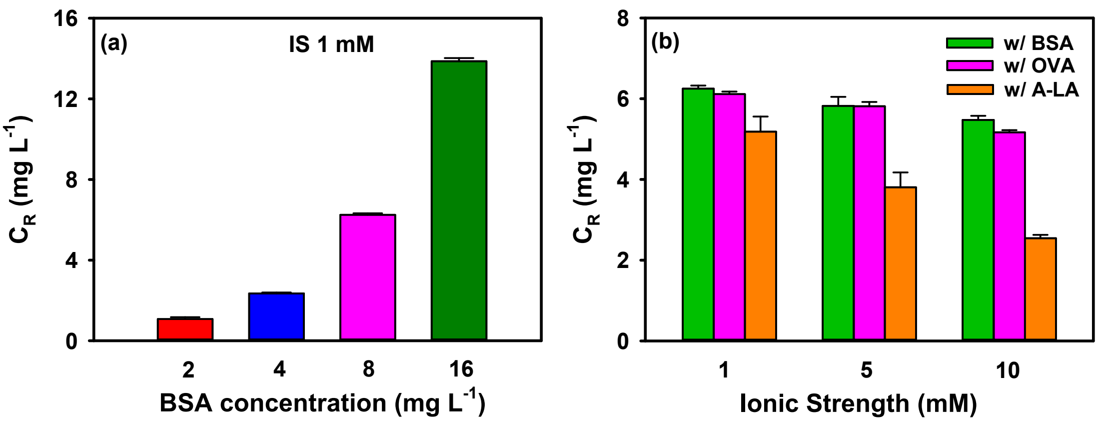

Fig. S9 Nonadsorbed protein in TiO2 suspension with different BSA concentrations (2, 4, 8, and 16 mg L^{-1}) at IS 1 mM, and nonadsorbed protein in TiO_2 suspension with 8 mg L^{-1} BSA, OVA, and A-LA at IS 1, 5, 10 mM.

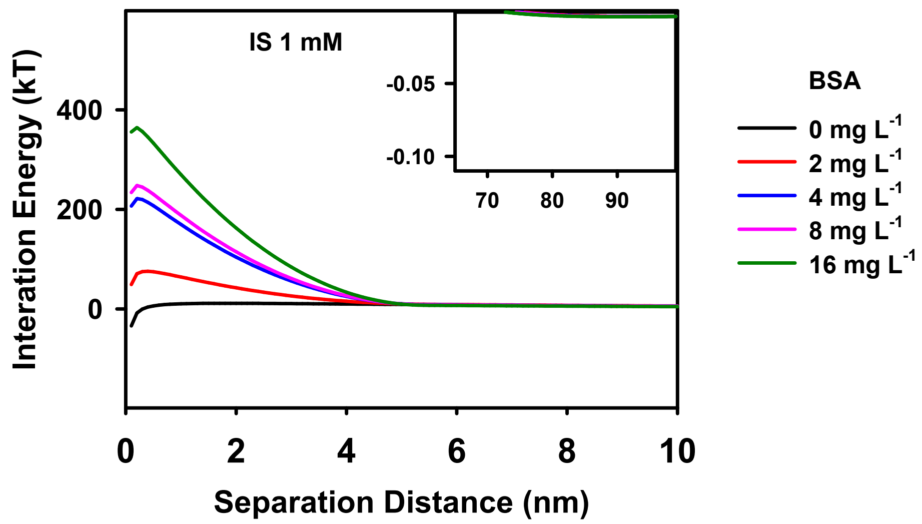

Fig. S10 Interaction energy profiles between grain surface and TiO_2 with BSA at IS 1 mM.

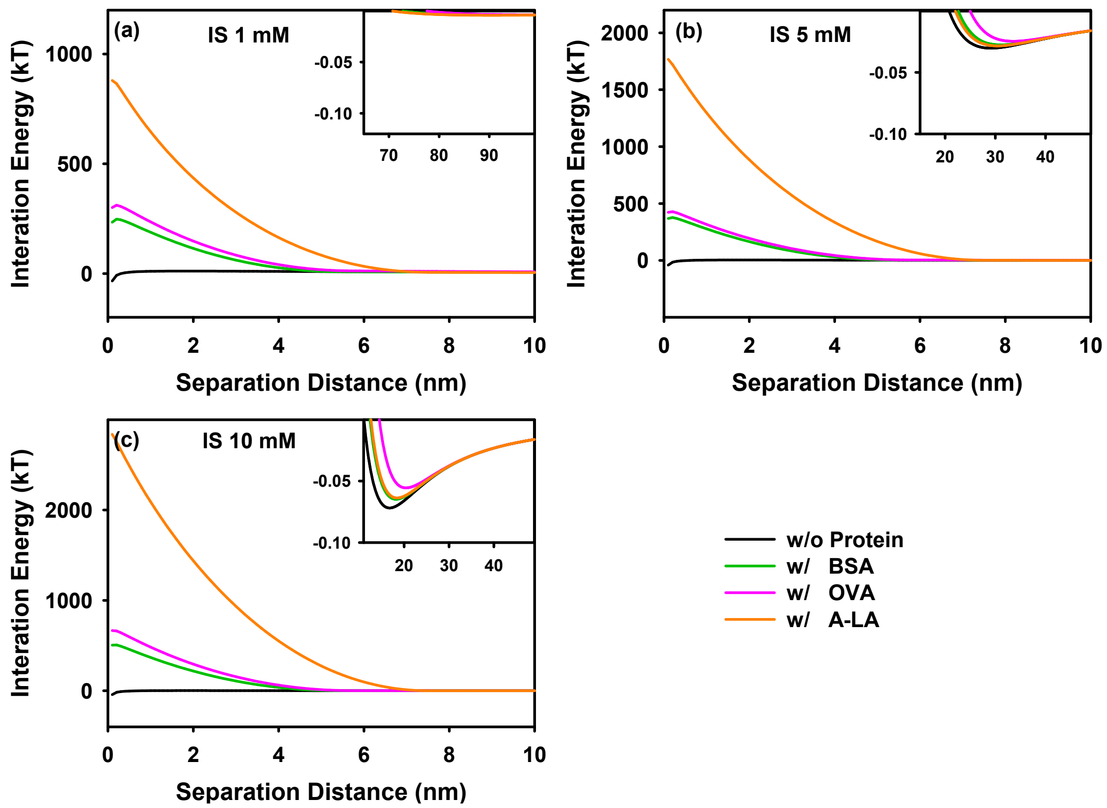

Fig. S11 Interaction energy profiles between grain surface and TiO_2 in the absence (w/o) and presence of 8 mg L^{-1} BSA, OVA, and A-LA at different IS.

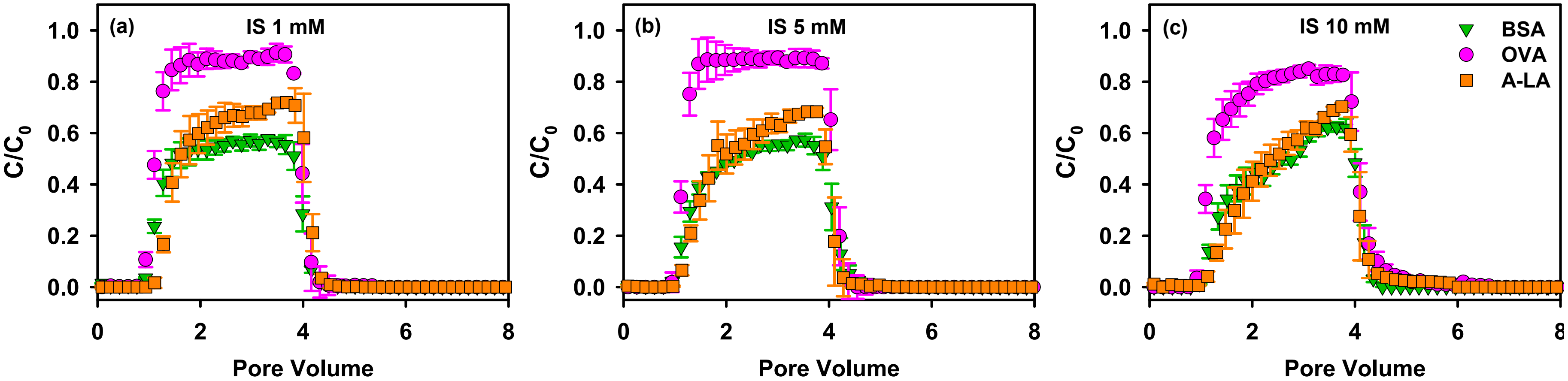

Fig. S12 Breakthrough curves for different protein at IS (a) 1, (b) 5, (c) 10 mM.

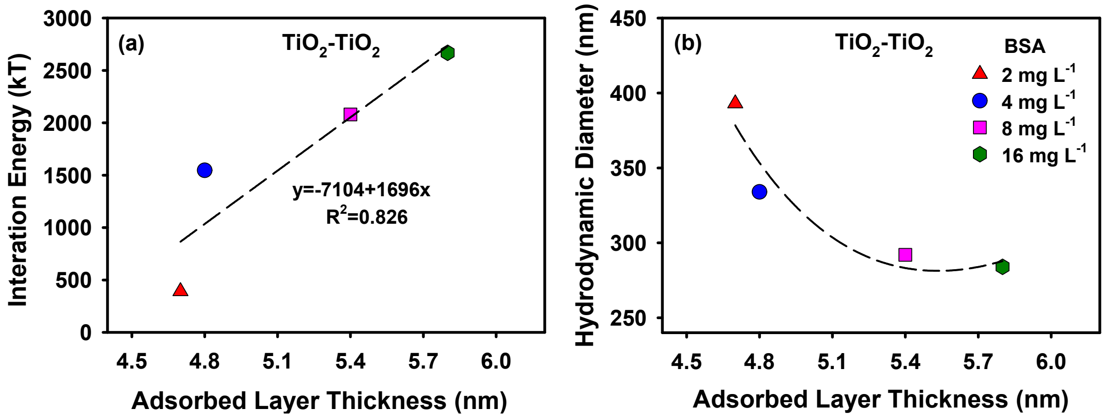

Fig. S13 The relationship between adsorbed layer thickness and (a) energy barrier or (b) hydrodynamic diameter, under TiO_2 with different BSA concentrations at IS 1 mM conditions.

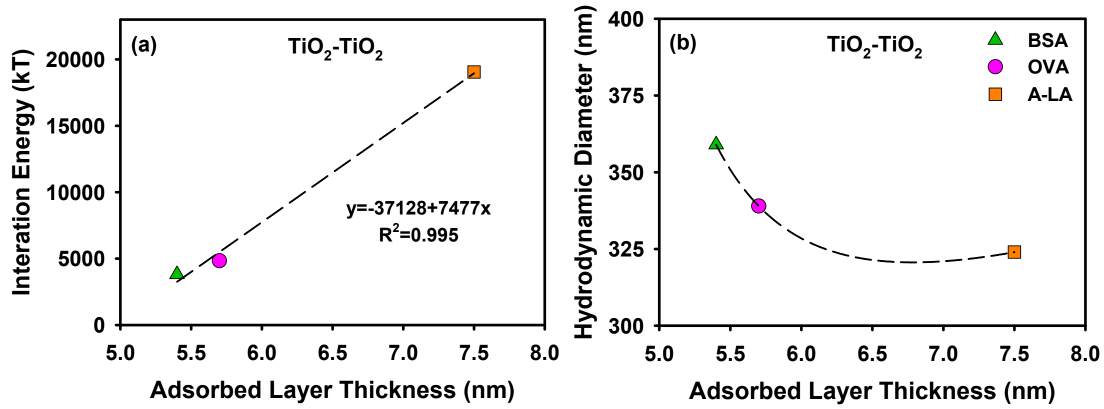

Fig. S14 The relationship between adsorbed layer thickness and (a) energy barrier or (b) hydrodynamic diameter under TiO_2 with different molecular weight proteins at IS 10 mM conditions.

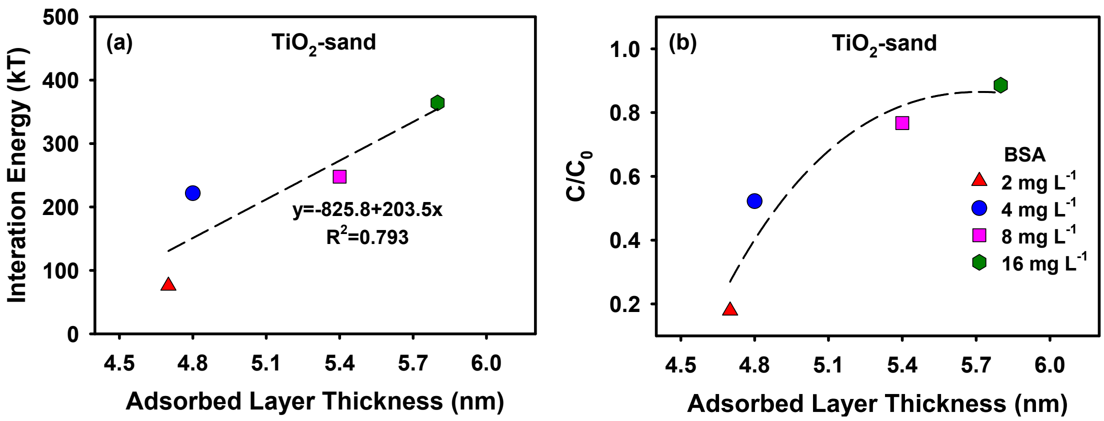

Fig. S15 The relationship between adsorbed layer thickness and (a) energy barrier or (b) breakthrough rates, under TiO_2 with different BSA concentrations at IS 1 mM conditions.

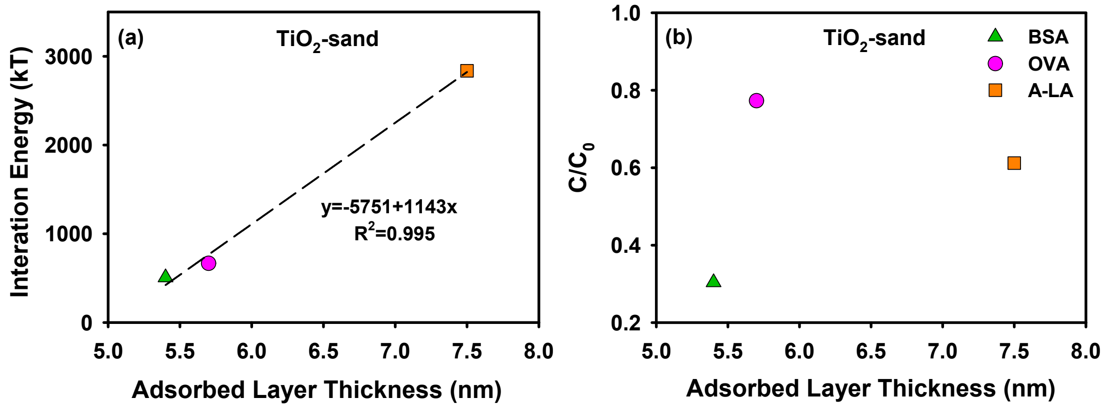

Fig. S16 The relationship between adsorbed layer thickness and (a) energy barrier or (b) breakthrough rates, under TiO_2 with different molecular weight proteins at IS 10 mM conditions.

Table S1 Hydrodynamic diameters (D_H) of TiO_2, TiO_2 with different BSA concentrations, and TiO_2 with different proteins in suspensions prior to and at the end of the column experiment.

IS (mM)	TiO_2 (mg L^{-1})	BSA (mg L^{-1})	OVA (mg L^{-1})	A-LA (mg L^{-1})	D_H (nm)		D_H/d_c [a]
					Prior to the experiment	End of experiment	
1	25	0	0	0	378 ± 10	3228 ± 159	0.0063
5	25	0	0	0	517 ± 25	4604 ± 235	0.0090
10	25	0	0	0	565 ± 13	4865 ± 169	0.0095
1	25	2	0	0	393 ± 18	411 ± 13	0.0008
1	25	4	0	0	334 ± 35	324 ± 9	0.0006
1	25	8	0	0	292 ± 9	277 ± 13	0.0006
1	25	16	0	0	284 ±20	286 ± 10	0.0006
1	25	0	8	0	253 ± 6	264 ± 7	0.0005
1	25	0	0	8	235 ± 13	253 ± 9	0.0005
5	25	8	0	0	296 ± 18	281 ± 10	0.0006
5	25	0	8	0	259 ± 31	276 ± 16	0.0005
5	25	0	0	8	249 ± 35	256 ± 13	0.0005
10	25	8	0	0	359 ± 31	401 ± 28	0.0008
10	25	0	8	0	339 ± 20	388 ± 23	0.0008
10	25	0	0	8	324 ± 8	389 ± 24	0.0008

[a] Ratio of average TiO_2 hydrodynamic diameter (D_H) at the end of column experiment over median grain size (d_c)

Table S2 Charge density (ZN/N_A), adsorbed layer thickness (d), and softness parameter ($1/\lambda$) are estimated by fitting electrophoretic mobility with the Ohshima's soft particle theory.

Particle	Protein type	Concentration (mg L^{-1})	ZN/N_A (mol m^{-3})	d (nm)	$1/\lambda$ (nm)	R^2
TiO_2	BSA	2	0.23	4.7	5.5	0.99
	BSA	4	0.33	4.8	5.1	0.99
	BSA	8	0.21	5.4	5.8	0.98
	BSA	16	0.35	5.8	5.6	0.99
	OVA	8	0.72	5.7	5.1	0.97
	A-LA	8	0.58	7.5	5.6	0.97